Sonochemical synthesis of nanostructured anatase and study of the kinetics among phase transformation and coarsening as a function of heat treatment conditions

Leonardo Gonzalez-Reyes [a],*, I. Hernández-Pérez [b], Francisco C. Robles Hernández [c],*, Héctor Dorantes Rosales [a], Elsa M. Arce-Estrada [a]

[a] *Instituto Politécnico Nacional, Departamento de Ingeniería Metalúrgica y Materiales, ESIQIE-UPALM, México, D.F. 07738, Mexico*
[b] *Universidad Autónoma Metropolitana-A, Departamento de Ciencias Básicas, Av. Sn. Pablo No. 180, México 02200, D.F., Mexico*
[c] *Transportation Technology Center Incorporated, Pueblo, CO 81001, USA*

Abstract

In the present paper are investigated the microstructural, phase transformation and coarsening kinetics of nanometric anatase subjected to different heat treatment conditions. It is also demonstrated that nanostructured anatase can be produced by a novel methodology assisted sonochemical means with the following particles characteristics; an average particle size of 6.2 nm and a specific surface area of $300 \, m^2 \, g^{-1}$. Sonochemically produced anatase subjected to heat treatments under ambient atmosphere conditions at temperatures from 773 K to 1073 K and times between 1 h and 72 h transforms only to rutile. Both rates, transformation to rutile and coarsening, increase with temperature. The critical size for the anatase particles to transform to rutile is temperature dependent. The coarsening kinetics, thus particle size, of the anatase and rutile investigated in this research can be predicted using exponential like equations. These equations are similar to the ones described in the LSW theory; in fact, the exponent changes as a function of time approaching 1/4 for times of 72 h of treatment. The characterization conducted in this research was assisted by means of Brunauer–Emmett–Teller (BET) method, thermo-gravimetric analysis (TGA), X-ray diffraction (XRD) and transmission electron microscopy (TEM). The characterization results are given and discussed herein.
© 2007 Elsevier Ltd. All rights reserved.

Keywords: Electron microscopy; Grain size; TiO₂; Functional applications; Sonochemical treatment

1. Introduction

The titanium dioxide (TiO₂) is found in nature with three crystalline structures with the following symmetries $D_{4h}^{14} - P4_2/mmm$ (tetragonal), $D_{4h}^{19} - I4_1/amd$ (body centered tetragonal) and $D_{2h}^{15} - Pcab$ (orthorhombic) for rutile, anatase and brookite, respectively. It has been reported that heat treatments applied to nanometric particles of anatase promote the phase transformation to rutile that is more stable at high temperatures and coarser grains.[1] Perhaps the number of well respected TiO₂

scientific publications there is no deep understanding about the coarsening of these phases that is a main focus of the present research. The phase transformation between anatase and rutile has been previously reported.[2–6] It has been suggested that phase transformation of anatase is highly dependent on the synthesis conditions such as temperature, purity of the components, texture, grain size, specific surface area, pore dimensions, among other characteristics.[2–6] Previous studies indicate that anatase has good characteristics for biological applications and has been successfully used as a reductor as well as for corrosive environments applications including photo-corrosion and chemical corrosion.[7–8]

The application of ultrasound methods to synthesize nanostructured materials has been successfully explored.[9] Ultrasound methods are capable of creating extreme conditions inside a

* Corresponding authors.
  E-mail addresses: leogonzalez@ipn.mx (L. Gonzalez-Reyes),
fcrh20@yahoo.com (F.C. Robles Hernández).

cavitating bubble, sponsoring cavitation to occur, and have shown positive effects to produce a variety of nanostructured materials.[10–11] Sonochemical synthesis is well known for increasing local temperatures and pressures combined with extraordinarily rapid cooling proving the required driving force for chemical reactions to occur under extreme conditions, which in many cases are ideal to produce nanometric or nanostructured materials. Sonochemical synthesis is a versatile method that can be satisfactorily used to produce nanostructured materials with different characteristics just by changing the treatment conditions (e.g. temperature, time, pH, etc.). Various applications for ultrasonic methods are used to enhance chemical reactivity and are easy to adapt for synthesis of nanometric materials and can be extrapolated for large scale production. Sonochemical decomposition of volatile organometallic precursors in low-volatile solvents produces nanometric materials in various forms and enhances their catalytic activity.[9]

The size of the nanometric TiO_2 have significant influence in the evolution of the phase transformation because their surface area have a positive contribution to the chemical potential or the driving force promoting the phase transformations to rutile or brookite.[12–13] The use of techniques such as sol–gel has been explore to produce amorphous TiO_2; finding that sol–gel products can be transformed to rutile and/or brookite using different heat treatment conditions.[13] Rutile can be obtained by heat treating anatase at temperatures as high as 1073 K.[1,14] Anatase is used for a wide range of applications as photocatalysis, solar energy conversion, protective surface coating, ceramics, etc.[14–18] Rutile is an effective light disperser and therefore, widely used for pigment.[19] Heat treatments promote the coarsening of anatase and/or rutile that can, in some cases, be beneficial for special applications.[20]

In the present work was used a novel methodology assisted by sonochemical synthesis to produce synthetic anatase. Sonochemical synthesis is capable of producing nanostructured anatase. The effects of heat treatment conditions on phase transformation (anatase–rutile), particle size, transformation times, temperature, lattice parameter, surface area and porosity were investigated and the results are presented and discussed herein.

2. Experimental

2.1. Synthesis and materials

Nanostructured anatase particles were synthesize using commercial grade substances; titanium tetraisopropoxide [(CH₃)₂CHO]₄Ti (97 wt% pure), acetone and methanol. Also, a mix of methanol and acetone (30 mL of each) was used as pressure-transmitting media and combined with 150 mL of titanium tetraisopropoxide. The mix was ultrasonically treated using a custom made ultrasonic bath equipped with a Branson transducer of 100 V, 30 W that generate pulses at a frequency of up to 38 kHz. The ultrasonic treatment was applied for a period of 50 min. After the sonochemical synthesis is concluded the products were dried in a magnetic mixer–heater at a temperature of 423 K. The drying process was conducted until the products
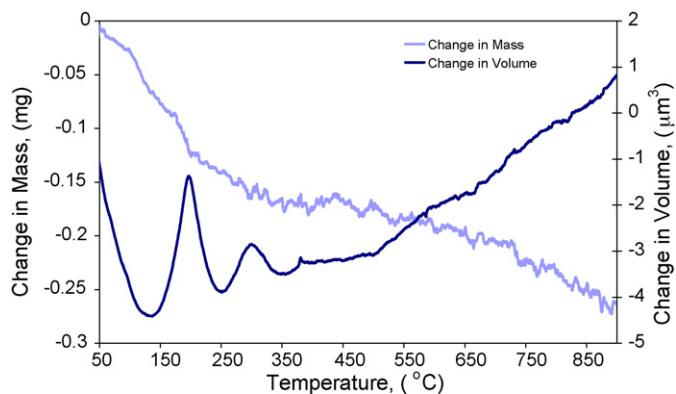

Fig. 1. Thermogravimetric analysis (TGA) showing weight and volume changes during the heating process on sonochemically produced anatase using a heating rate of $10\,K\,min^{-1}$.

had a liquid free, thus dry, appearance. The dried product was identified as synthetic anatase and is refer along this paper as original sample.

2.2. Heat treatment

The synthesized anatase (original sample) was heat treated at 773 K, 873 K, 973 K and 1073 K in a conventional electric resistance furnace in open air atmosphere. The treatments were carried out for times varying between 1 h and 72 h.

2.3. Characterization methods

The X-ray diffraction (XRD) characterization was conducted on a Bruker D8 Discover apparatus that operates under θ–2θ conditions the samples were scanned from $20°$ to $60°$, 2θ. The XRD characterization was conducted using a Cu Kα tube with a characteristic wavelength (λ) of 0.15405 nm. For the XRD was used a scanning speed of $2°$/min with readings collected every $0.02°$. The systematic error of the XRD apparatus is approximately 0.188% that is considered negligible. The X-ray patterns were indexed to identify the phases present. The Scherrer equation (Eq. (1)) was used to determine the particle size of the original and heat treated samples.[21] The following planes (1 0 1) and (1 1 0) were used to determine the particle size for anatase and rutile, respectively. The lattice parameter and lattice volume of anatase and rutile were determined using the XRD peaks (1 0 1) and (2 0 0) for anatase and (1 1 0) and (2 1 1) for rutile.

$$D = \frac{K\lambda}{\beta^{1/2}\mathrm{Cos}\theta} \tag{1}$$

where D is the average diameter of the particle; K is the shape factor of the average particle (for this study a shape factor of 0.9 was used); λ is the wavelength characteristic of Cu ($\lambda = 0.15405$ nm) and $\beta^{1/2}$ is the width of the X-ray peak at half its high, for anatase and rutile the respective (1 0 1) and (1 1 0) planes were used, as per reference [29] the corresponding planes are located at $\theta = 12.65°$ and $\theta = 13.72°$.

The weight fraction of anatase (W_A) and rutile (W_R) for the samples heat treated at 873 K, 973 K and 1073 K was
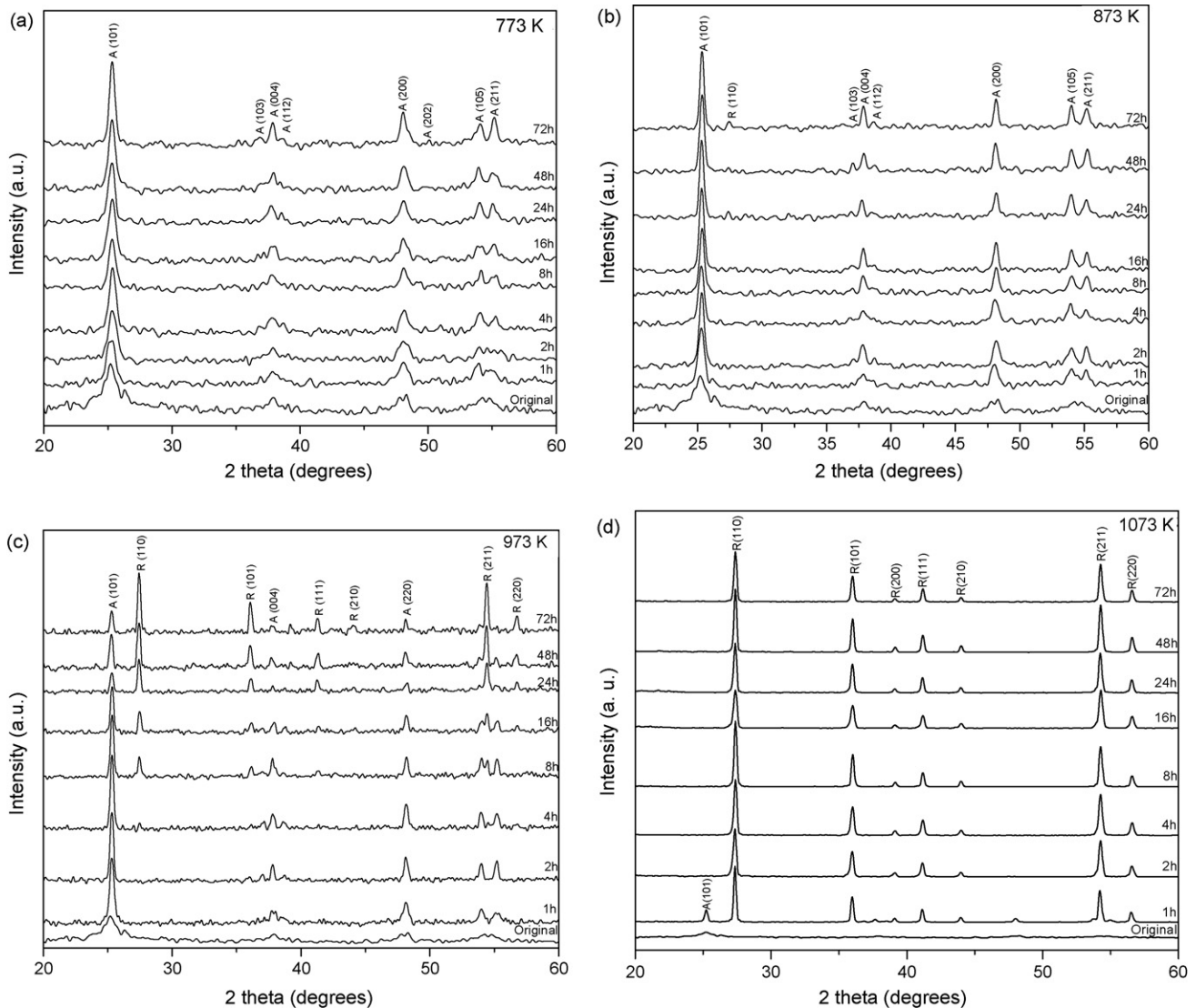
Fig. 2. X-ray diffraction (XRD) patterns of the original powders and heat treated powders at various times for temperatures of (a) 773 K, (b) 873 K, (c) 973 K and (d) 1073 K.

determined using the Spurr–Meyers method[22] the equations are provided in following:

$$W_A = \frac{1}{[1 + 0.8(I_A/I_R)]} \qquad (2)$$

$$W_R = \frac{1}{[1 + 1.26(I_R/I_A)]} \qquad (3)$$

where I_A and I_R are the peaks intensities in c.p.s. for the (1 0 1) plane for anatase and (1 1 0) plane for rutile.

The transmission electron microscopy (TEM) analysis was conducted on a JEOL-2000FXII operated at 200 kV. The TEM analysis includes diffraction patterns, dark fields and bright fields. Using TEM was determined the crystalline structure, morphology, coarsening kinetics and the results are used to support the XRD findings.

The specific surface area of the original sample was measured using BET on a Micrometrics ASAP 2000 nitrogen adsorption apparatus. Prior to the BET analysis, the sample was degassed

and aged at 373 K for 24 h. The adsorption analysis was conducted using nitrogen with relative pressures (P/P_0) between 0.5 and 1.0. P indicates the equilibrium pressure among the gas and the solid and P_0 is the pressure of the gas required for the saturation at the temperature of the experiment.

The thermogravimetric analysis (TGA) was performed on a Stanon Redcroft STA 1640 apparatus with a heating rate of 10 K min^{-1}. The reference sample used during the absorption process aid the determination of the band-gap energy using a Varian Cary I spectrophotometer.

3. Results

Table 1 shows the characteristics of the original anatase as obtained from the sonochemical synthesis. The measured area using BET was of 300.3 m^2 g^{-1} with a grain size of 6.2 nm as determined by XRD-Scherrer. The band-gap shown in Table 1 is 5.3% lower than the value reported in reference 14 sug-

gesting that sonochemically produced anatase has potential for applications such as biological, photo-corrosion, chemical corrosion, and environmental applications. Still further analyses are required to determine the areas 24 where the sonochemically produced anatase can be applied.

Fig. 1 shows the TGA results where is observed a change in mass during the heating sequence of the original powders. The change in mass occurs at temperatures below 573 K. Prior to the TGA, it was decided not to heat the original powders above 423 K with the aim to preserve their characteristics. For that reason during the heating TGA sequence changes in mass and volume are identified at temperatures of 573 K or lower. These changes are consistent with the removal of remaining organic substances from the sonochemical synthesis. Above 573 K these changes are negligible; however, the change in volume is the result of densification of the heat treated powders, it means a reduction in the pore volume and surface area. Similar changes in mass and volume were previously reported by Reidy et al.[4] The TGA results indicate that there is no mass change involved during the phase transformation between anatase and rutile, which is expected since both phases have the same stoichiometry.

Fig. 2 shows the XRD patterns of the samples heat treated at different temperatures and times. In all cases the heat treatments were conducted using reference anatase powders. In the XRD pattern at 773 K high background intensity is observed, that can be the result of a high density of defects, pores and potentially amorphous matter.[23] The analysis of the XRD sequence shows a reduction in the width of the XRD peaks for anatase and rutile and a shift to the right of the anatase peaks as the time of the heat treatment increases for temperatures of 773 K and 973 K. The increase in the intensity of the peaks of anatase and rutile as a function of time and temperature can be deduced by comparing the XRD patterns for the different heat treatment conditions to the original sample. The above is potentially attributed to the increase in crystal quality as the heat treatment time and temperature increases. On the other hand, rutile is first identified in the heat treated sample at 873 K for 24 h, which is presumably formed from coarsened anatase particles resulting in the more stable location for the XRD rutile peaks.

Fig. 3 shows the Scherrer analysis as a function of time for the different heat treatment temperatures and represents the coarsening kinetics of anatase and rutile. As can be observed in Fig. 3 samples heat treated for more than 8 h, show a quasi-linear coarsening. Therefore, the transformation and coarsening rate were determined for temperatures and times larger than 8 h. In all cases a high regression coefficient was obtained ($R^2 \geq 0.88$). The coarsening of all heat treated samples at the different temperatures follow a continuous path where the size of both, anatase and rutile, increases as a function of time except for anatase heat treated at 873 K for more then 24 h and 973 K for more than 4 h.
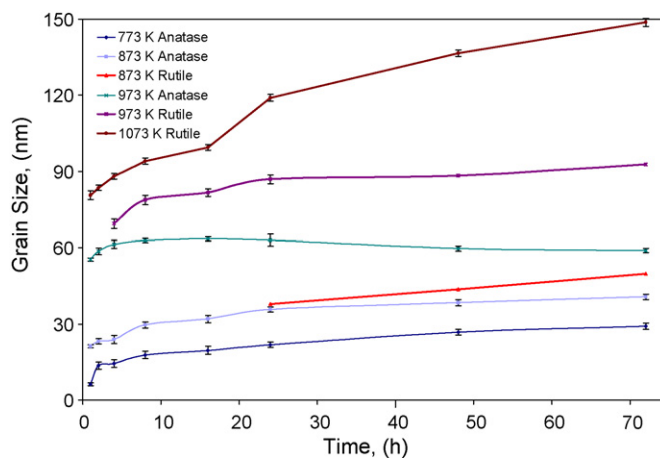

Fig. 3. Coarsening of anatase and rutile as calculated by Scherrer from the XRD patterns for the various heat treatment times and temperatures.

For the above temperatures and times the respective coarsening rates decreased; it is of particular interest the samples heat treated at 973 K for more than 16 h that present a drop in particle size.

It is literally impossible that the particles of anatase shrink as the heat treatment time increases, perhaps what the curve suggest is that coarser anatase particles are more susceptible to transform to rutile. It means the coarse anatase particles reach its critical size for transformation and automatically transform to rutile. The larger anatase particles lead the formation of rutile because this phase is thermodynamically more stable at larger particle size and higher temperatures. This is agreement with the fact that for the same heat treatment conditions rutile particles are always coarser than the anatase ones as indicated by the particle size results obtained the Scherrer equation (Fig. 3). It is also observed that grain coarsening has an almost negligible effect on the grain size range (indicated by error bars); in fact, for some heat treatment conditions the error bars are not visual indicating how narrow grain size range is. This agrees with the narrow width of the XRD anatase (1 0 1) and rutile (1 1 0) peaks (Fig. 2).

Table 2 shows the phases present for the different heat treatment temperatures, the transformation rates, coarsening rates and the coarsening kinetic exponential equations. The equations presented in Table 2 are the regression equations of the curves shown in Fig. 3 from 1 h to 72 h and from 8 h to 72 h. It is clear that the coarsening rate for the heat treated sample at 873 K and 973 K is considerably reduced by the phase transformation, recommending that coarsening and phase transformation are not independent processes. For the above-mentioned temperatures, phase transformation and coarsening are processes that occur simultaneously; however, all anatase particles that reach

Table 1

Microstructural characteristics of the reference simple after the synthesis of the TiO_2 powders

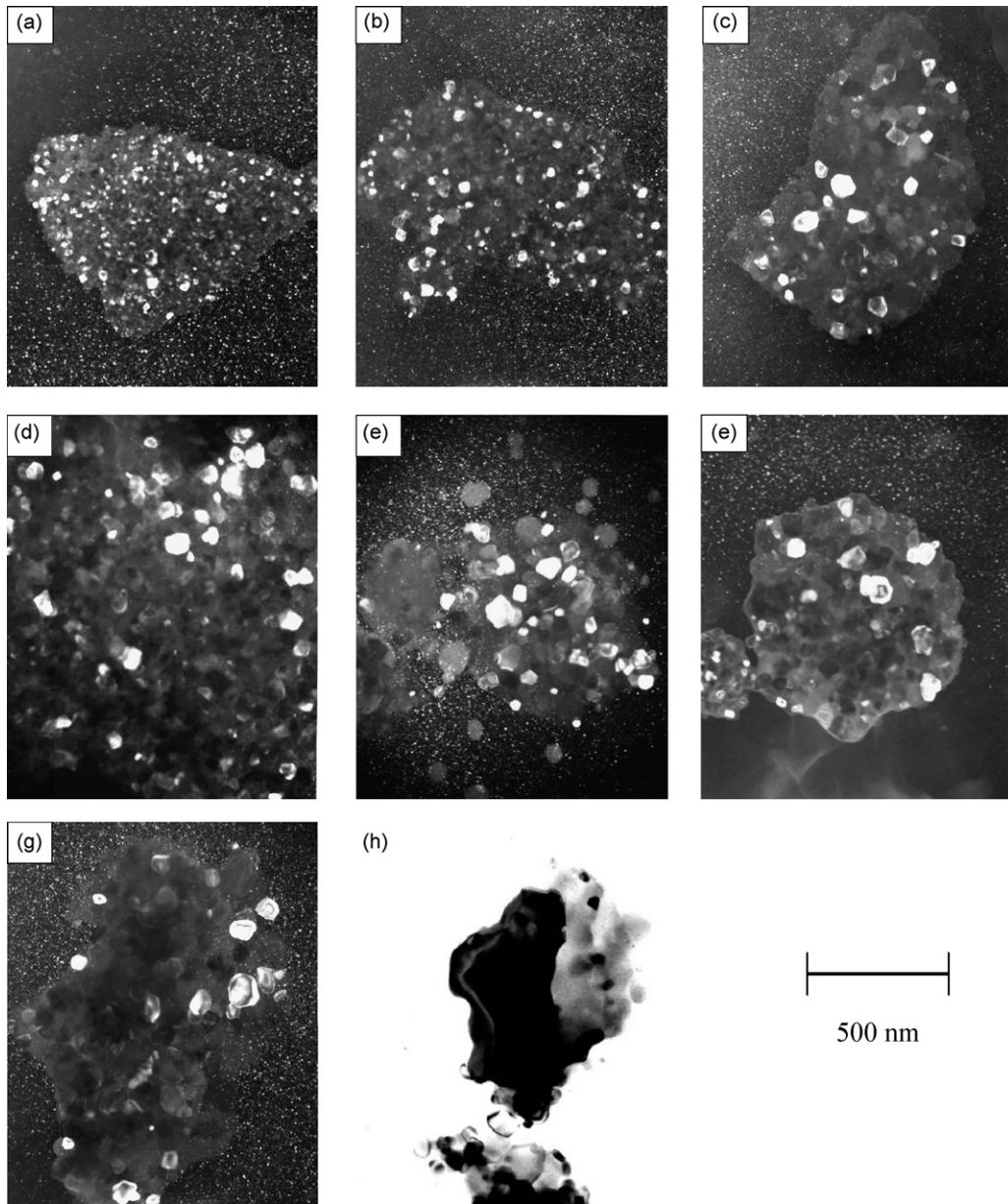|	Phase	Crystallite size (nm)		BET area ($m^2\,g^{-1}$)	Pore volume ($cm^3\,g^{-1}$)	Average pore (nm)	Band gap (eV)
		TEM	Scherrer				
Original	Anatase	5.4 ± 2.5	6.2	300.31	0.34	3.82	3.03

Fig. 4. TEM micrographs showing the coarsening kinetics of anatase nanoparticles heat treated at temperature of 873 K for (a) 1 h, (b) 2 h, (c) 4 h, (d) 8 h, (e) 16 h, (f) 24 h, (g) 48 h and (h) 72 h.

Table 2
Coarsening analysis of anatase and rutile at diferent temperatures as determined from XRD

Treatment temperature (K)	Phases	Lattice parameter (nm)		Transformation rate (%/h)	Coarsening rate (nm/h)
		1–72 h	8–72 h		
773	Anatase	$D_{anat} = 13t_{500}^{0.208}$	$D_{anat} = 12.1t_{500}^{0.229}$	0	0.20
873	Anatase	$D_{anat} = 20.6t_{600}^{0.161}$	$D_{anat} = 21.7t_{600}^{0.148}$	0.11	0.17
	Rutile	$D_{rutile} = 17.4t_{600}^{0.242}$	$D_{rutile} = 17.4t_{600}^{0.242}$		0.78
973	Anatase	$D_{anat} = 58.5t_{700}^{0.014}$	$D_{anat} = 68.8t_{700}^{-0.034}$	0.23	−0.06
	Rutile	$D_{rutile} = 67.5t_{700}^{0.073}$	$D_{rutile} = 67.5t_{700}^{0.073}$		0.22
1073	Rutile	$D_{rutile} = 74.4t_{800}^{0.145}$	$D_{rutile} = 57.4t_{800}^{0.222}$	87	0.86

D and t are the crystallite diameter and the heat treatment time at the respective temperature. The 1–72 h and 8–72 h indicate the time ranges where the regression was conducted.
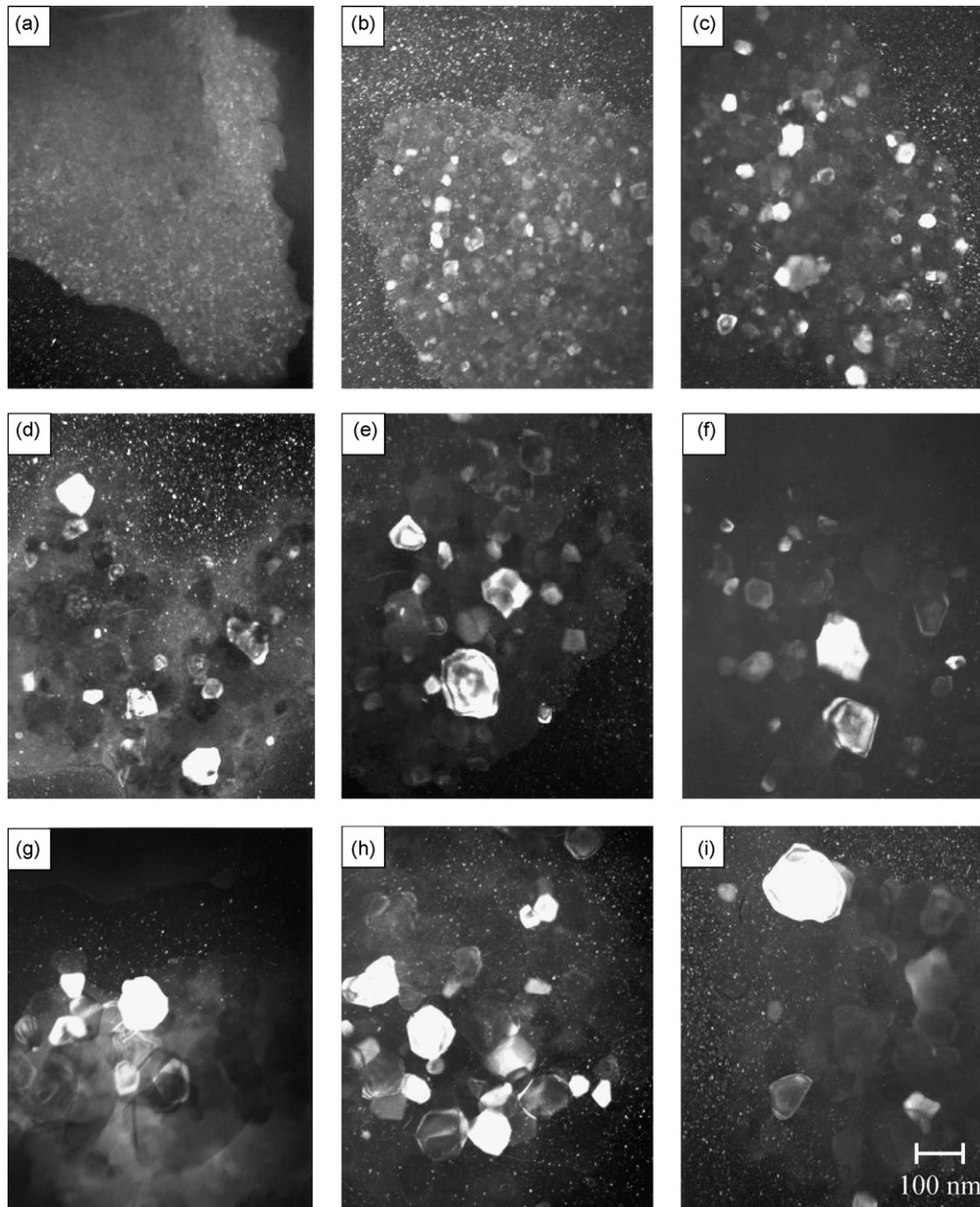
Fig. 5. TEM micrographs showing the coarsening of nanometric anatase particles heat treated at 973 K for (a) 0 h, (b) 1 h, (c) 2 h, (d) 4 h, (e) 8 h, (f) 16 h, (g) 24 h, (h) 48 h and (i) rutile for 72 h.

its critical size cannot longer coarse and are forced to transform to rutile. The coarsening kinetic exponential equations clearly show a decrease in the exponent for the curves of anatase at the temperatures (873 K and 973 K) that correspond to the time where anatase continuously transforms to rutile. Another important aspect to consider on the coarsening kinetic equations is that the exponent for the equations for times from 1 h to 72 h of heat treatment is smaller than for times above 8 h. The main reason is that as time increases the coarsening rate tapers off approaching the typical Lifshitz, Slyozov and Wagner (LSW) exponent value of $\alpha = 1/3$. This exponent value is characteristic of long and ideally "infinite" heat treatment times. Using the coarsening kinetic equations in Table 2 it is possible to predict the time

at a particular temperature required to reach a desired particle size for anatase and/or rutile. Equations in Table 2 are limited to determine the particle size for heat treated anatase between 1 h and 72 h and temperatures from 773 K to 1073 K. Future efforts are focused in the development of a more sophisticated equation(s) capable of the prediction of the anatase/rutile ratio and the particle size for a broader range of temperatures and times.

Figs. 4 and 5 show two TEM coarsening sequences for anatase heat treated at 873 K and 973 K, respectively. Fig. 4 focuses in the coarsening of anatase illustrating a clear coarsening path of such phase, which further confirms the Scherrer results (Fig. 3). On the other hand, Fig. 5 shows micrographs of heat treated anatase except for Fig. 5i that correspond to rutile. From Fig. 5f
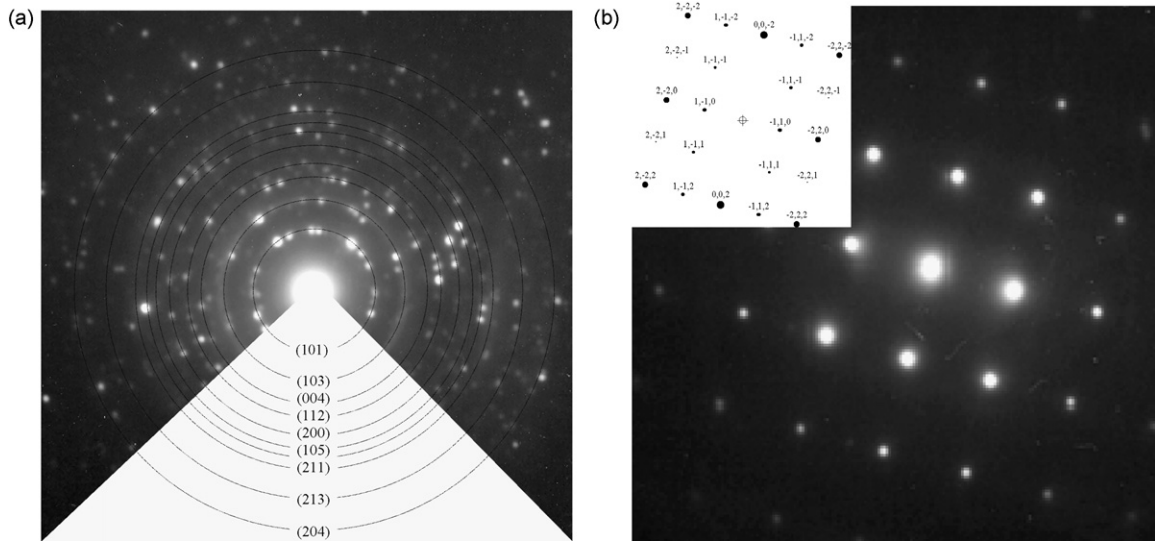
Fig. 6. Indexed selected area electron diffraction patterns (SAEDP) for (a) anatase and (b) rutile.

to h it is clear that anatase does not coarse any further, this is in agreement with the results shown in Fig. 3. Moreover, Fig. 5i confirms the fact that rutile particles continue their coarsening as a function of temperature and it can be observed that rutile particles are coarser than the ones of anatase.

Fig. 6 shows the indexed selected area electron diffraction patters (SAEDP) for anatase and rutile. The analysis of the SAEDP of the original sample confirms that the only phase present after synthesis is anatase, while the SAEDPs of samples heat treated for more than 2 h at 1073 K indicate that the only phase present is rutile. From the SAEDP can be deducted that anatase is a nanostructured phase since the SAEDP is an arrangement of diffused rings while the size of the particles for rutile are larger resulting in a spots-like SAEDP.

Both, anatase and rutile, have rombohedric crystalline structures consequently they have different values for the lattice parameters "a and c". In Fig. 7a and b are plotted the respective lattice parameters for anatase and rutile for the different heat treatments temperatures. For anatase "a" decreases and "c" increases for times of 8 h or less and for more than 8 h the lattice parameter is more stable this is consistent for the investigated temperatures.

Fig. 7b shows that the lattice parameters, "a" and "c", for rutile are almost constant, for the investigated heat treatment times and temperatures. This is attributed to the fact that rutile particles were formed from the already coarsened anatase particles. Therefore, larger particles correspond to higher crystallinity that results in a more stable lattice parameter for the transformed rutile. These findings are in full agreement with the SAEDP as well as the results shown in Fig. 3. More important is that the lattice parameters of rutile for the sample heat treated at 1073 K are larger than the lattice parameters of the heat treated sample at 973 K.

In Fig. 8 is presented the change in lattice volume for anatase and rutile as a function of heat treatment time. The lattice volume for anatase particles show variation for heat treated samples for short times (<8 h) and is more stable in samples heat treated
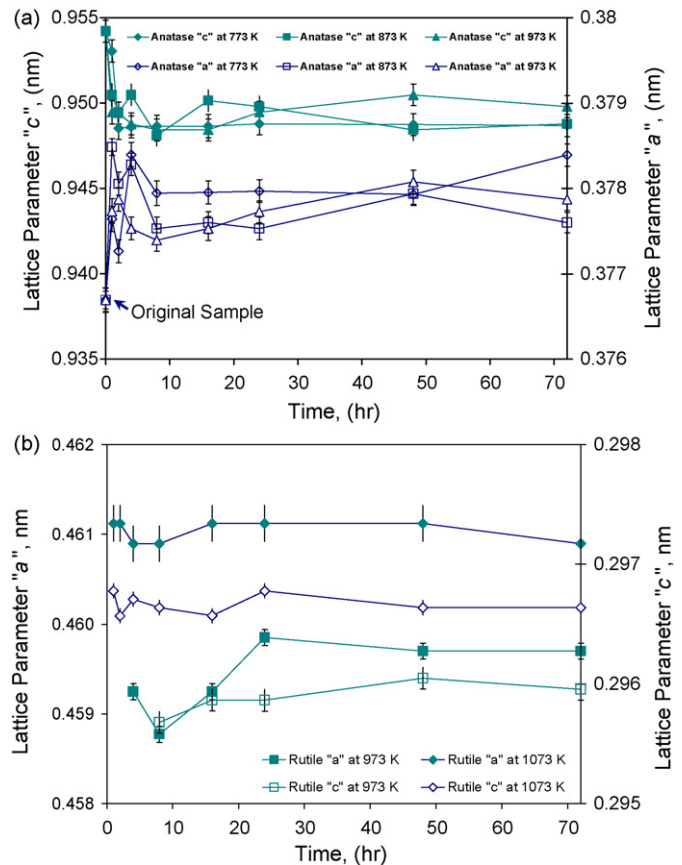

Fig. 7. Changes in lattice parameters for (a) anatase and (b) rutile for various heat treatment temperatures.

for more than 8 h, which is in agreement with the "a and c" lattice parameter variation. At the same time and for short heat treatment times a lattice volume change is observed; probably attributed to the higher ratio of crystalline defects vs. the atoms in the lattice. Such ratio decreases for longer heat treatment times and is apparently independent of the heat treatment tempera-
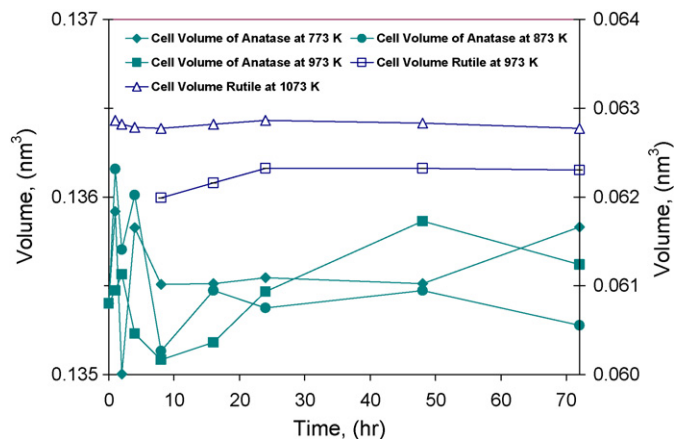
Fig. 8. Change in lattice volume of anatase and rutile as a function of heat treatment temperature and times.

ture. The same behavior is observed in all cases for anatase heat treated at the investigated temperatures. In contrast for rutile the changes in lattice volume is not apparent showing an almost constant lattice volume for the samples heat treated at 973 K and 1073 K, except for the small increase observed in lattice volume for the heat treated samples at 973 K between 8 h and 24 h.

The respective lattice parameters for anatase and rutile are $a_{anatase} = 0.3785$ nm and $c_{anatase} = 0.9514$ nm and $a_{rutile} = 0.4593$ nm and $c_{rutile} = 0.2959$ nm as reported in reference 29. The difference for the heat treated samples in lattice volume for anatase is between 0.1 and 0.7% from the smallest to the largest lattices with respect to the theoretical value and 0.6% between the smallest and the largest lattice values for the original and heat treated anatase. For rutile these differences vary from −0.7% to 0.7% with respect to the theoretical volume for the smallest and the largest lattices identified. For the respective lattice volume of rutile the heat treated sample at 1073 K is 1.4% larger than the sample heat treated at 973 K.

4. Discussion of the results

Anatase heat treated at 773 K coarsens approximately 2.5 times than anatase heat treated at 873 K. Anatase heat treated at 873 K and 973 K show a clear reduction in coarsening rate attributed to the phase transformation to rutile. Furthermore, the coarsening rate of rutile when heat treated at 1073 K is approximately 7.4 times larger than anatase heat treated at 973 K. It is important to point out that the coarsening rate was determined using linear regressions for times between 8 h and 72 h.

The anatase on the samples heat treated at 773 K did not transform after 72 h; in contrast, 86.5% of the anatase transformed to rutile in 1 h for samples heat treated at 1073 K. The coarsening of the particles as determined by Scherrer went from 6.2 nm for the original sample to 29.1 nm when heat treated 773 K for 72 h and to 71.9 nm for the heat treated sample at 1073 K for 1 h. Rutile was firstly identified after 24 h of heat treatment at 873 K with a particle size of 37.9 nm and after 1 h when heat treated at 1073 K with a particle size of 80.6 nm and a maximum size of 148.7 nm after 72 h. The above-mentioned coarsening val-

ues are in agreement with results previously reported in the literature.[12,25] At 973 K and 72 h only 77.48% is transformed to rutile and at 1073 K, 100% of anatase is transformed to rutile in less than 2 h. Comparing the particle size of anatase and rutile can be concluded that for higher temperatures larger particle sizes are required for the phase transformation to rutile to be initiated.

The coarsening mechanism can be analyzed as two kinetic domains, in the first domain anatase has two functions, (1) coarse and (2) transform to rutile, in the second domain rutile is identified and has the sole function of coarsening. Both domains, when analyzed separately for anatase at 773 K and rutile at 1073 K is observed an Ostwald ripening like behavior[26] in particular for heat treatment times between 8 and 72 h (Table 2). In the coarsening mechanism, the smaller particles of anatase coalesce on bigger ones sponsoring their growth; it means mass transfer occurs from the smaller to the larger anatase particles promoting their coarsening and thus their instability. As a result a reduction in the number of particles is observed (Figs. 4 and 5). However, the size of the remaining particles of both, anatase and rutile, increase except for the heat treated samples at 973 K where the heat treatment conditions sponsor the phase transformation over the coarsening of anatase. Such results can be observed in the XRD patterns by the reduction in the width of the peaks as the heat treatment time increases or by direct examination of Figs. 4 and 5. Two main conclusions can be drawn (1) the rate of transformation anatase–rutile increases with temperature and (2) coarsening and phase transformation are not independent mechanisms.

The transformation of anatase to rutile at high temperatures suggests that rutile is more stable at higher temperatures and coarser particles that is in full agreement with references 12–17,30–38. The heat treatments times and temperatures investigated in the present research indicate that the amount of anatase and rutile as well as the grain size can be precisely controlled to obtain a particular ratio of phases and with specific particle size.

Based on the previous analysis it can be observed that the critical particle size at which anatase transforms to rutile varies. For example, at 873 K anatase particles, when they transformed for the first time to rutile (24 h) reached a critical size of 35.7 nm. At 973 K the critical size for the anatase to rutile transformation is 61.3 nm after 4 h of treatment and the heat treated samples at 1073 K initiate their transformation in less than 1 h with a size <71.9 nm. On the other hand, the maximum size reached by the anatase particles was 71.9 nm and 148.7 nm for rutile; these sizes were identified in the heat treated samples at 1073 K for 1 h and 8 h, respectively.

There are two important aspects in the above described coarsening-transformation kinetics, (1) the critical size of the particle for transformation and (2) the coarsening of the transformed rutile particles. Due to the critical size for the anatase to rutile transformation, anatase particles that reach this size transform to rutile impeding any further coarsening of anatase and at the same time the newly formed rutile particles initiate their coarsening.

The driving force for the phase transformation (anatase–rutile) is the thermodynamic instability of the

coarsened anatase particles at the particular heat treatment temperature as reported in references 30–38. However, the size and temperatures at which anatase particles transform to rutile in the present research is not in complete agreement with the results reported in references 30–38, which is attributed to the differences of the original powders due to the distinct synthesis methods used.[2,6] The results of this research indicate that anatase can be produced and artificially coarsened to particular crystalline size that can be predicted using the respective coarsening exponential equations given in Table 2.

The difference in the critical particle size for the transformation of anatase is attributed to large density of point and line defects. The coarsening of the particles is diffusion controlled and the transformation is controlled by the thermodynamic instability of anatase. Therefore, in order for the anatase to transform to rutile a critical radius of anatase, with a minimum of defects, is required and since surface diffusion is higher than the intergranular diffusion for higher temperatures the coarsening of the particles is promoted over their transformation. This results in the observed difference in critical size for transformation of the anatase.

5. Coarsening kinetics

The analysis of the results in the present research indicates three major processes that are in agreement with the Ostwald ripening theory.[26–28] The coarsening of the particles of anatase or rutile show the following:

  (i) mass conservation,
 (ii) a continuity coarsening evolution as a function of time and size distribution,
(iii) growth of the individual particles of given size

The mass conservation can be demonstrated in Fig. 1. The coarsening is demonstrated in Fig. 3 and equations in Table 2 and the growth and reduction in the number of particles is confirmed in Figs. 4 and 5. The Ostwald ripening theory does not considered phase transformations or the multi-particle diffusion. Therefore, a theory that more closely described the effect of the phase transformation of a second phase is the LSW[26–29] and the multi-particle diffusion effect is better described in the Voorhees–Glicksman model.[27]

The exponent (α) of the coarsening equations from Table 2 can be analyzed separately for the entire coarsening process (1–72 h) and for times larger than 8 h. Times between 8 h and 72 h provide a more realistic analysis of the coarsening kinetics, since at the beginning of the heat treatment a fast rate of coarsening is observed and after 8 h this rate become more stable for all the heat treated samples. The exponents for the equations shown in Table 2 (heat treated samples at 773 K, 873 K and 1073 K) for regressions between 1 h and 72 h is in all cases between $\alpha = 1/5$ and $1/7$ and for times from 8 to 72 h and the exponent increases to approximately $\alpha = 1/4$. The $\alpha = 1/4$ is closer to the traditional $\alpha = 1/3$ LSW value,[26] thus it is expected that for longer heat treatment times α will approach 1/3. This will allow the modeling of the coarsening kinetics of anatase and rutile using an LSW-like equation for any time and temperature.

6. Conclusions

In the present research was found that this novel sonochemical method is capable of producing nanostructured particles of anatase. Anatase is sensitive to phase transformation when heat treated at different temperatures and times producing rutile particles of different sizes. The heat treatment conditions can be controlled to produce either pure rutile or a combination of anatase–rutile with specific particle sizes. Using a mathematical model similar to the LSW, it is possible to predict the size of the particle for heat treated anatase and rutile. The coarsening process can be described using the Oswald ripening approach; however, more detailed theories that fully describe the coarsening kinetics of anatase (produced by sonochemical means) and rutile are the LSW and Voorhees–Glicksman.

The phase transformation has a direct influence in coarsening kinetics allowing to conclude that both are not independent processes. Heat treatments sponsor at first the coarsening of anatase particles, but once the anatase particles reach a critical size (with a minimum of point and linear defects) the phase transformation is initiated. Therefore, At this point the only anatase particles that coarsen are the smaller ones. The lattice parameters of rutile are more stable than the ones for anatase and this is independent of the heat treatment conditions. The reason for this is that rutile is formed from coarse anatase particles that have a higher crystal quality with less defects and thus more stable lattice parameters.

References

 1. Kumar, K. P., *Scr. Metall. Mater.*, 1995, **32**, 873.
 2. Kumar, K. N. P., Keizer, K. and Burggraaf, A., *Nature*, 1992, **358**, 48.
 3. Park, H. K., Kim, D. K. and Kim, C. H., *J. Am. Ceram. Soc.*, 1998, **80**, 743.
 4. Reidy, D. J., Holmes, J. D. and Morris, M. A., *J. Eur. Ceram. Soc.*, 2006, **26**, 1527.
 5. Burns, A., Hayes, G., Li, W., Hirvonen, J., Demaree, J. D. and Shah, S. I., *Mater. Sci. Eng. B*, 2004, **111**, 150.
 6. Gamboa, J. A. and Pasquevich, D. M., *J. Am. Ceram. Soc.*, 1992, **75**, 2934.
 7. Al-Salim, N. I., Bagshaw, S. A., Bittar, A., Kemmitt, T., Maquillan, A. J., Mills, A. M. and Ryan, M. J., *J. Mater. Chem.*, 2000, **10**, 2358.
 8. Ito, S., Inoue, S., Kawada, H., Hara, M., Iwaski, M. and Tada, H., *J. Colloid Interface Sci.*, 1999, **216**, 59.
 9. Kennet, S., Suslick and Gareth, *J. Price. Annu. Rev. Mater. Sci.*, 1999, **29**, 295–326.
10. Grinstaff, M. W., Cichowlas, A. A., Choe, S. B. and Suslick, K. S., *Ultrasonics*, 1992, **30**, 168.
11. Suslick, K. S., Fang, M., Hyeon, T. and Cichowlas, A.A., Molecularly design nanostructure materials, *MRS Symp. Proc.*, 1994, **351**, 443.
12. Gribbs, A. A. and Banfield, J. F., *Am. Mineral.*, 1997, **82**, 717.
13. Lottici, P. P., Bersani, D., Braghini, M. and Montero, A., *J. Mater. Sci.*, 1993, **28**, 177.
14. Gouma, P. I. and Mills, M. J., *J. Am. Ceram. Soc.*, 2001, **84**, 619.
15. Hoffmann, M. R., Martin, S. T., Choi, W. and Bahnemann, W. D., *Chem. Rev.*, 1995, **95**, 69.

16. Cai, R., Kubota, Y., Shuin, T., Hashimoto, K. and Fujishima, A., *Cancer Res.*, 1992, **52**, 2346.
17. Gan, J. Y., Chang, Y. C. and Wu, T. B., *Appl. Phys. Lett.*, 1998, **72**, 332.
18. Fujishima, A., Rao, T. N. and Tryk, D. A., *J. Photochem. Photobiol. C: Photochem. Rev.*, 2000, **1**, 1.
19. Braun, J. H., *Coat. J. Technol.*, 1997, **69**, 59.
20. Li, W., Ni, C., Lin, H., Huang, C. P. and Shan, S. I., *J. Appl. Phys.*, 2004, **96**, 11.
21. Cullity, B. D. and Stock, S. R., *Elements of X-Ray Diffraction*. Prentice Hall, New Jersey, 2001.
22. Spurr, R. A. and Myers, H., *Anal. Chem.*, 1957, **29**, 760.
23. Eastman, J. A., *J. Appl. Phys.*, 1994, **75**, 770.
24. DeLoach, J. D., Scarel, G. and Aita, C. R., *J. Appl. Phys.*, 1999, **85**, 2377.
25. JiUian, F., Banfield, A., Brian, L., Bischoff, B., Marc, A. and Anderson, A., *Chem. Geol.*, 1993, **110**, 211.
26. Voorhees, P. W., *Annu. Rev. Mater. Sci.*, 1992, **22**, 197.
27. Voorhees, P. W. and Glicksman, M. E., *Acta Metall.*, 1984, **32**,2013.
28. Henrich, V. E. and Cox, P. A., *The Surface Science of Metal Oxides*. Cambridge University Press, Cambridge, UK, 1994.
29. XRD tables, JCPDS-International Centre for Diffraction Data, 84-1286 (anatase) and 87-0920 (rutile).
30. Bladan, A., *J. Mater. Sci.*, 2002, **37**, 2171.
31. Penn, R. L. and Banfield, J. F., *Am. Mineral.*, 1998, **83**, 1077.
32. Shannon, R. D., *J. Appl. Phys.*, 1964, **35**, 3414.
33. Diebold, U., *Surface Sci. Rep.*, 2003, **48**, 53.
34. Xie, H., Zhang, Q., Xi, T., Wang, J. and Liu, Y., *Thermochimica Acta*, 2002, **381**, 45.
35. Kim, B. K. and Choi, C. J., *Scripta Mater.*, 2001, **44**, 2161.
36. Ding, X. Z. and Liu, X. H., *J. Mater. Sci. Lett.*, 1996, **15**, 1789.
37. Kholmanov, I. N., Barborini, E., Vinati, S., Piseri, P., Podesta, A., Ducati, C., Lenardi, C. and Milani, P., *Nanotechnology*, 2003, **14**, 1168.
38. Ihara, T., Moyoshi, M., Iriyama, Y., Matsumoto, O. and Sugihara, S., *App. Catal. Environ.*, 2003, **42**, 403.